

Supporting Information:

NMRlipids IV: Headgroup & glycerol backbone structures, and cation binding in bilayers with PS lipids

Pavel Buslaev,[†] Fernando Favela,[‡] Tiago M. Ferreira,[¶] Ivan Gushchin,[†] Matti Javanainen,[§] Batuhan Kav,^{||} Jesper J. Madsen,[⊥] Markus Miettinen,^{||} Josef Melcr,[§] Ricky Nencini,[§] O. H. Samuli Ollila,^{*,§} and Thomas Piggot **Authorlist is
not yet complete[®]**

[†]*Moscow Institute of Physics and Technology*

[‡]*Mexico*

[¶]*Halle, Germany*

[§]*Institute of Organic Chemistry and Biochemistry, Academy of Sciences of the Czech Republic, Prague 6, Czech Republic*

^{||}*Department of Theory and Bio-Systems, Max Planck Institute of Colloids and Interfaces,
14424 Potsdam, Germany*

[⊥]*Department of Chemistry, The University of Chicago, Chicago, Illinois 60637, United States of America*

[#]*Institute of Biotechnology, University of Helsinki
@Southampton, United Kingdom*

E-mail: samuli.ollila@helsinki.fi

S1 Simulated systems

S1.1 CHARMM36

POPC bilayer. Previously published values²⁴ calculated from the data available from Ref. 25 are used.

DOPS and POPS bilayers.

The data in Table I and Refs 26–28 T. Piggot, please write simulation details

POPC:POPS mixtures without additional ions

Simulations of POPC:POPS (5:1) mixture containing total 132 (110:22) lipids with potassium and sodium counterions were ran using CHARMM36 force field. The data are available from Refs. 5 and 8, respectively T. Piggot, please write simulation details.

Simulations of POPC:POPS (5:1) and POPC:POPS (1:1) mixtures containing total 300 lipids with potassium counterions were ran using CHARMM36 force field. The data are available from Refs. 4 and 29 J. Madsen, please write simulation details.

POPC:POPS (5:1) mixtures with additional monovalent ions. POPC:POPS (110:22) mixtures containing total 132 lipids with the additional potassium or sodium ions corresponding concentrations of ~450 mM and 890 mM were generated with the CHARMM-GUI.^{30,31} Systems were simulated using Gromacs 5³² and CHARMM36 force field with the simulation parameters given by the CHARMM-GUI at 298 K. For further details, simulation files and data, see table S1 and Refs. 6,7,9,10.

POPC:POPS (5:1) mixtures with additional calcium

POPC:POPS (5:1) mixtures containing total 300 (250:50) lipids were simulated with the additional calcium concentrations. The data is available from Refs. 33 and 34. J. Madsen, please write simulation details.

Table S1: The list of POPC:POPS mixtures simulated with different amounts of added monovalent ions. The salt concentrations are calculated as [salt]= $N_c \times [\text{water}] / N_w$, where [water]=55.5 M. This corresponds the concentration in buffer before solvating lipids, which are reported in the experiments by Roux et al.¹ The simulation details are given in the supplementary information.

lipid/counter-ions	force field for lipids / ions	^a C _{ci} (M)	^b N _i	^c N _w	^d N _c	^e T (K)	^f t _{sim} (ns)	^g t _{anal} (ns)	^h files
POPC:POPS (5:1)/K ⁺	CHARMM36 ^{2,3}	0	250:50	11207	0	298	200	180	4
POPC:POPS (5:1)/K ⁺	CHARMM36 ^{2,3}	0	110:22	4620	0	298	500	100	5
POPC:POPS (5:1)/K ⁺	CHARMM36 ^{2,3}	0.45	110:22	4926	40	298	200	150	6
POPC:POPS (5:1)/K ⁺	CHARMM36 ^{2,3}	0.89	110:22	4946	79	298	200	150	7
POPC:POPS (5:1)/Na ⁺	CHARMM36 ^{2,3}	0	110:22	4620	0	298	500	100	8
POPC:POPS (5:1)/Na ⁺	CHARMM36 ^{2,3}	0.44	110:22	4965	39	298	200	150	9
POPC:POPS (5:1)/Na ⁺	CHARMM36 ^{2,3}	0.89	110:22	4932	79	298	200	150	10
POPC:POPS (5:1)/K ⁺	MacRog ¹¹	0	120:24	5760	0	298	400	250	12
POPC:POPS (5:1)/K ⁺	MacRog ¹¹	0.50	120:24	5760	52	298	300	200	13
POPC:POPS (5:1)/K ⁺	MacRog ¹¹	1.00	120:24	5760	104	298	300	200	13
POPC:POPS (5:1)/K ⁺	MacRog ¹¹	2.00	120:24	5760	208	298	300	200	13
POPC:POPS (5:1)/K ⁺	MacRog ¹¹	3.00	120:24	5760	311	298	300	200	13
POPC:POPS (5:1)/K ⁺	Lipid14/17 ^{14,15}	0	120:24	5760	0	298	500	200	16
POPC:POPS (5:1)/K ⁺	Lipid14/17 ^{14,15}	0.50	120:24	5760	54	298	300	200	17
POPC:POPS (5:1)/K ⁺	Lipid14/17 ^{14,15}	1.00	120:24	5760	104	298	300	200	17
POPC:POPS (5:1)/K ⁺	Lipid14/17 ^{14,15}	2.00	120:24	5760	208	298	300	200	17
POPC:POPS (5:1)/K ⁺	Lipid14/17 ^{14,15}	3.00	120:24	5760	311	298	300	200	17
POPC:POPS (5:1)/K ⁺	Lipid14/17 ^{14,15}	4.00	120:24	5760	415	298	300	200	17
POPC:POPS (5:1)/Na ⁺	Lipid14/17 ^{14,15}	0	120:24	5760	0	298	500	200	18
POPC:POPS (5:1)/Na ⁺	Lipid14/17 ^{14,15}	0.50	120:24	5760	54	298	300	200	19
POPC:POPS (5:1)/Na ⁺	Lipid14/17 ^{14,15}	1.00	120:24	5760	104	298	300	200	19
POPC:POPS (5:1)/Na ⁺	Lipid14/17 ^{14,15}	2.00	120:24	5760	208	298	300	200	19
POPC:POPS (5:1)/Na ⁺	Lipid14/17 ^{14,15}	3.00	120:24	5760	311	298	300	200	19
POPC:POPS (5:1)/Na ⁺	Lipid14/17 ^{14,15}	4.00	120:24	5760	415	298	300	200	19
POPC:POPS (4:1)/Na ⁺	Berger ^{20,21}	0	102:26	4290	0	310	120	80	22
POPC:POPS (4:1)/Na ⁺	Berger ^{20,21}	1.03	102:26	4290	80	310	200	50	23

^aExcess Na⁺ or K⁺ concentration

^bNumber of lipid molecules with largest mole fraction

^cNumber of water molecules

^dNumber of additional cations

^eSimulation temperature

^fTotal simulation time

^gTime used for analysis

^hReference for simulation files

S1.2 CHARMM36ua

DOPS and POPS bilayers.

The data in Table I and Refs 35,36 T. Piggot, please write simulation details

S1.3 MacRog

POPC bilayers. The POPC bilayer consisting of a total of 128 lipids was constructed from single lipid structure taken from Ref. 37. The bilayer was hydrated by a total of 5120 water molecules, corresponding to 40 water molecules per lipid. The MacRog lipid parameters,³⁸ obtained from Ref. 37, were used, along with the TIP3P water model.³⁹ The simulation parameters were identical to those used for POPC/POPC mixtures with the MacRog force field, see below. The simulation was run for 200 ns using Gromacs 2016.3,⁷ out of which 150 ns were used for analyses. The simulation data and related files are available from Ref. 40.

POPS bilayers.

The data in Table I and Refs 41,42 T. Piggot and M. Javanainen, please write simulation details

Piggot: please write about system with Na⁺ counterions.

This membrane was further simulated after replacing Na⁺ counterions by K⁺ ones, which were described by the Åqvist parameters.⁴³ Other topologies were unchanged. The simulation parameters were the same as used for the POPC/POPS mixtures with the MacRog force field, see below. The simulation was run for 200 ns, out of which 150 ns was used in the analyses.

POPC:POPS (5:1) mixtures with additional potassium ions

The data in Table II and Refs 12,13

The bilayers containing a total of 120 POPC and 24 POPS molecules distributed evenly among the two leaflets were set up using CHARMM-GUI.^{30,31} The bilayers were solvated by 5760 water molecules, corresponding to 40 water molecules for lipid. Additionally, 24 potassium ions were added to neutralize the charge of the POPS head groups. These bilayers were simulated using Gromacs ??⁷ in the presence of counterions only, as well as together with different concentrations of CaCl₂ or KCl. For the former, concentrations of 100 mM, 300 mM, 1 M, and 3 M were considered, which corresponded to the amounts of 10/20, 31/62, 104/208, and 311/622 of Ca²⁺/Cl⁻ ions. For membranes with KCl, concentrations of 500 mM, 1 M, 2 M, and 3 M were considered, corresponding to 52, 104, 208, or 311 pairs of K⁺ and Cl⁻ ions.

The lipids were described using the MacRog model.^{11,38,44} The POPC topologies were obtained from Ref. 37, whereas the POPS topology was adapted from Ref. 44. Notably, the chains were reversed in order to modify OPPS into POPS. Unlike the D stereoisomer present in Ref.,⁴⁴ the POPS head group conformations generated by CHARMM-GUI are in the naturally occurring L stereoisomer. TIP3P model³⁹ was used for water, and the Åqvist parameters,⁴³ standard for the OPLS force field, were employed for the ions.

The simulation parameters were taken from Ref. 44. Periodic boundary conditions were employed in all dimensions. The list of neighbors was updated every step I used nstlist=1 because it's used in the mdp in the article quoted. In DOI: 10.1021/jp5016627, nstlist=10 is used. The Lennard-Jones interactions were cut off at 1 nm, whereas the smooth particle mesh Ewald algorithm⁴⁵ was used for electrostatics. Dispersion correction⁴⁶ was applied to both energy and pressure. Temperature was kept constant at 298 K using the Nosé–Hoover thermostat.^{47,48} The lipids and the solvent were coupled separately, and a time constant of 0.4 ps was employed. Pressure was maintained semi-isotropically at 1 bar using the Parrinello–Rahman barostat with a time constant of 1 ps.⁴⁹ All non-water bonds were constrained with the LINCS algorithm,^{50,51} whereas the bonds in water molecules were constrained using SETTLE.⁵² The integration time step was set to 2 fs, and the simulations were performed

either for 400 ns (only counterions), 300 ns (systems with KCl), or 600 ns (systems with CaCl₂). The last 250, 200, or 300 ns of the simulations were included in the analyses, respectively.

S1.4 Lipid17

DOPS and POPS bilayers.

The structure of the bilayers with 128 DOPS or 128 POPS lipids were obtained from CHARMM-GUI.^{30,31} Bilayers are solvated with 4480 water molecules resulting in 31.1 water molecules per lipid. For each system, 128 NaCl molecules are added to neutralize the system.

Each bilayer structure was first minimized for 2500 steps with steepest descent and an additional 2500 step with the conjugent gradient algorithms while restrainig the solvent and ion molecules with a force constant 500 kcal mol⁻¹ Å⁻¹. An additional minimization step was used with the same parameters after removing the constraints on the solvent and ion molecules. During the minimization procedure, non-periodic boundary conditions were applied, no pressure scaling was used and none of the bonds were restrained. A three step heating procedure was applied: in the first heating step the system temperature is increased from 0.0 K to 100.0 K using Langevin thermostat with 5.0 ps⁻¹ collision frequency while restraining the lipid positions with harmonic springs of force constant 20.0 kcal mol⁻¹ Å⁻¹ at constant volume without periodic boundary conditions. In the second heating step, the system temperature was increased from 100.0 K to 200.0 K using Langevin thermostat with 5.0 ps⁻¹ collision frequency within 10000 steps while restraining the lipid positions with harmonic springs of force constant 10.0 kcal mol⁻¹ Å⁻¹ at constant volume. In the third heating step, the system temperature is increased from 200.0 K to 303.0 K within 10000 steps using Langevin thermostat with 5.0 ps⁻¹ collision frequency while restraining the lipid positions with harmonic springs of force constant 10.0 kcal mol⁻¹ Å⁻¹ at 1 bar constant

pressure using Berendsen barostat with 3.0 ps relaxation time. From the second heating step onward, periodic boundary conditions in all dimensions were applied. The semi-isotropic pressure coupling along *xy*-plane was employed and the surface tension was set to 0.0 dyn explicitely. After the third heating step, each structure is equilibrated for 100 ns at 1 bar and 303 K constant pressure using Berendsen barostat and temperature using Langevin thermostat, respectively. For the equilibration step, semi-isotropic pressure coupling along *xy*-plane was employed and the surface tension was set to 0.0 dyn explicitely. For all heating and equilibration steps, the lengths of the hydrogen containing bonds were restrained using SHAKE algorithm and a time step of 2 fs was used. In all steps with periodic boundary conditions, the non-bonded interactions are calculated with particle mesh Ewald⁴⁵ using 1.0 nm cutoff.

For the production runs, the temperature and pressure were set to 303 K and 1 bar, using Langevin thermostat with 1.0 ps⁻¹ collision frequency and Berendsen barostat with 1.0 ps relaxation time, respectively. Periodic boundary conditions were applied in all dimensions and the non-bonded interactions are calculated with particle mesh Ewald⁴⁵ using 1.0 nm cutoff. The lengths of the hydrogen containing bonds were constrained using SHAKE algorithm and a time step of 2 fs was used. Trajectories are saved in every 10 ps intervals. Two independent trajectories of 500 ns long was generated and the last 200 ns portions were used for the analysis.

In all simulations, TIP3P⁵³ was used as the solvent. SETTLE⁵² algorithm was employed to constrain the bonds in TIP3P water molecules. Simulations were ran using Amber18 simulation package? Is this correct, do we need the citation? and lipid parameters were obtained from Amber Lipid17 force field.¹⁵ For the ions, one set of simulations were run with Joung-Cheatham ion parameters⁵⁴ and one set of simulations were run with ff99SB⁴³ ion parameters. The data in Table I and Refs 55–58 contain the details of the simulations and the raw trajectories, respectively.

POPC:POPS (5:1) mixtures with additional potassium and sodium ions

The initial structure of the bilayers with 120 POPC and 24 POPS lipids were obtained from CHARMM-GUI.^{30,31} Bilayers were solvated with 5760 TIP3P water molecules.⁵³ For the simulations of the lipids and ions, the Amber Lipid 17¹⁵ and ff99SB⁴³ force fields were used, respectively. Simulations were ran using Amber18 simulation package? Is this correct, do we need the citation? The simulation steps are the same as the the simulations of DOPS and POPS bilayers described above, with the only difference that the total simulation time was 300 ns, of which last 200 ns was used for the analysis. The number of ions in each specific system is given in Table S1. The trajectory files can be found in Refs 16–19.

POPC:POPS (5:1) mixtures with additional calcium

The data in Table II and Refs 59,60

One set of simulations of POPC:POPS (5:1) mixtures with additional calcium ions has been performed using Amber18 simulation package. Number of ions and water molecules for this set of simulations are shown in Table II. The simulation details, minimization, heating, and equilibration runs are the same as described above for the other POPC:POPS (5:1) simulations with Amber Lipid17 forcefield. For all simulations, ff99SB⁴³ ion parameters and Amber lipid 17 force field were used. For each ion concentration, 100 ns equilibration runs were followed by 300 ns production runs with two independent trajectories, of which last 200 ns were used for the analysis. The trajectory files can be found in Ref 60

J. Melcr, please write simulation details

S1.5 Berger

POPC bilayers. Previously published simulation⁶¹ available from Ref. 62 was used for POPC at 310 K.

DOPS and POPS bilayers.

The data in Table I and Refs 63,64 T. Piggot, please write simulation details

POPC:POPS (4:1) mixtures with additional sodium and calcium ions. Previously published simulations with the additional amount of sodium⁶⁵ available from Ref. 23 and with the additional amounts of calcium⁶⁶ available from Refs. 67,68 were used. The additional sodium ions were removed from the structure file of the simulation with excess amount of sodium²³ to generate the initial structure for the reference simulation with sodium counterions only. The data, input and force field parameter files of the reference simulation are available from Ref. 22. The simulation details of this are not clearly described in Zenodo repository, but can be read from the mdp file available there. Should we write the detailes here or not?

S1.6 GROMOS-CKP and GROMOS-CKPM

CKPM refers to the version with Berger/Chiu NH₃ charges compatible with Berger (i.e. the NH₃ group having the same charges as in the N(CH₃)₃ group of the PC lipids; 'M' stands for Mukhopadhyay after the first published Berger-based PS simulation that used these charges²¹) and CKP refers to the version with more Gromos compatible version (i.e. the charges for the NH₃ group taken from the lysine side-chain). T. Piggot, please write the description of force field.

DOPS and POPS bilayers.

The data in Table I and Refs. 69–72 T. Piggot, please write simulation details

POPC:POPS (5:1) mixtures without additional ions

The data in Table II and Refs. 73,74 T. Piggot, please write simulation details

S1.7 Slipids

DOPS and POPS bilayers.

The data in Table I and Refs. 75–77. T. Pigget and F. Favela, please write simulation details

S2 Electrometer concept in PC lipid bilayers mixed with negatively charged lipids

The electrometer concept is based on the empirical observations that the order parameters of α and β carbons in PC lipid headgroup decrease (increase) proportionally to the bound positive (negative) charge^{78–81} (Fig. S1). Therefore, the headgroup order parameters can be used to measure the ion binding affinity to lipid bilayers containing PC lipids.^{1,78–80,82,83} Changes of the headgroup order parameters of negatively charged PS and PG lipids are also systematic, but less well characterized.^{1,82–84} Therefore, the ion binding affinity to negatively charged bilayers can be better characterized measuring the PC headgroup order parameters from mixed bilayers.^{1,82–85}

When using the PC headgroup order parameters to evaluate the ion binding affinity to a bilayer containing anionic lipids, it is important to note that the order parameters increase due to the addition of negative charged lipids according to the electrometer concept^{80,86} (Fig. S1). Therefore, the PC headgroup order parameters are larger in mixtures with anionic lipids than in pure lipid bilayers. This is evident also in the headgroup order parameters of POPC in bilayers with different amounts anionic lipids without added calcium (Fig. S2). Upon addition of CaCl_2 , the order parameters decrease and reach the values of pure PC bilayer close to the CaCl_2 concentrations of $\sim 50\text{-}300\text{mM}$, depending on the amount of negatively charged lipids in the mixture (Fig. S2). Around these concentrations the positive charge of bound Ca^{2+} cancels the negative charge lipids, resulting to a neutral membrane. Above such concentrations, the specific binding of calcium leads to the overcharging of the membrane.

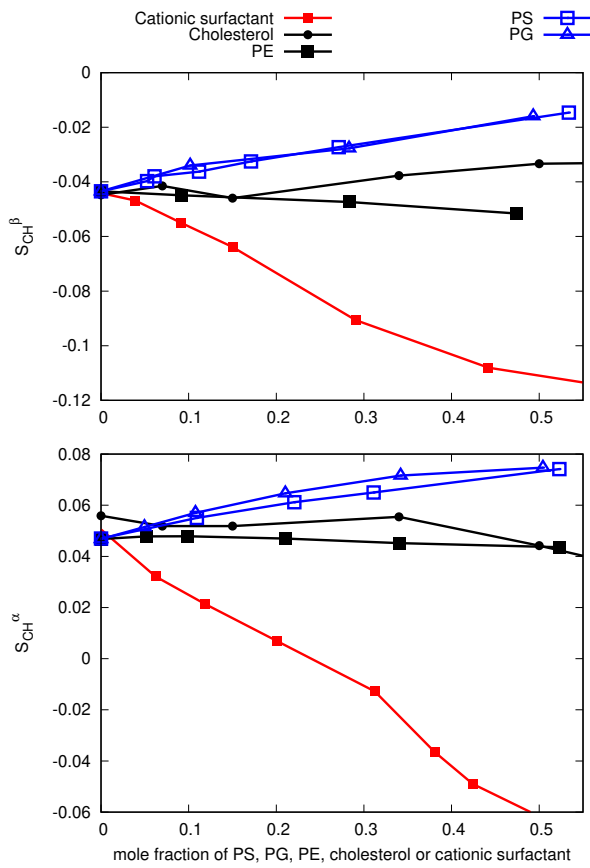


Figure S1: Headgroup order parameters of POPC measured from mixtures with PS (bovine brain), POPG, POPE, cholesterol and cationic dihexadecyldimethylammonium bromide (DHAB) surfactant.^{81,86,87} Signs are taken from separate experiments.^{88,89}

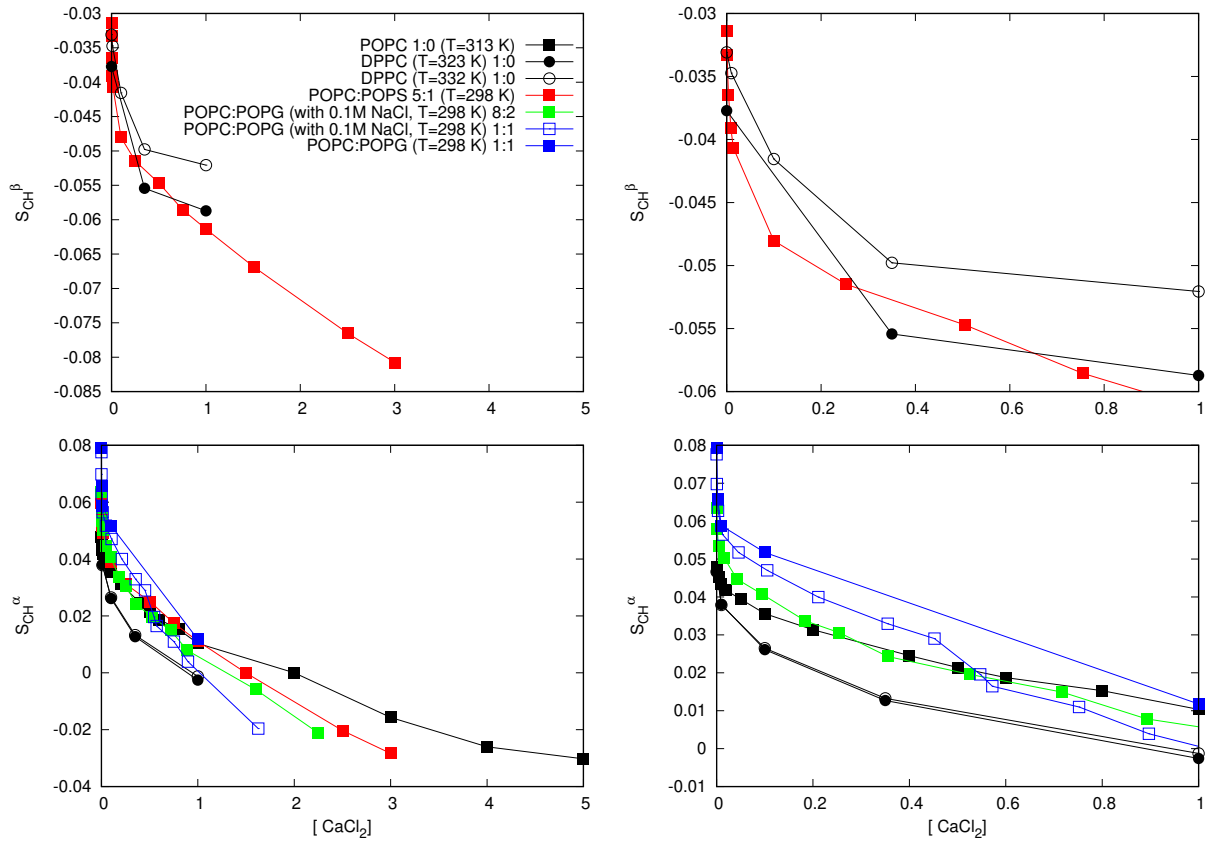


Figure S2: Headgroup order parameters of POPC as a function of CaCl_2 concentration from experiments with different mole fractions of negatively charged lipids (left column). Right column shows the same data zoomed to the concentrations below 1M. Data for Pure DPPC from Ref. 78, for pure POPC from Ref. 79, for POPC:POPS (5:1) mixture from Ref. 1, for POPC:POPG (8:2,1:1) mixtures with 0.1M NaCl from Ref. 83 and for POPC:POPG (1:1) mixture data without NaCl from Ref. 82.

Because the POPC headgroup order parameters in mixtures with different amounts of anionic lipids but without additional salt are not equal, the binding affinity of calcium can be better compared by plotting the changes of order parameters as a function of added calcium. As expected, such a plot reveals more pronounced order parameter decrease in systems with larger fractions of negatively charged lipids (Fig. S3), indicating an increase in the calcium binding affinity with the increasing amount of negatively charged lipids in membranes. In conclusion, the presented empirical comparison of headgroup order parameter changes from various mixtures of POPC and anionic lipids with added calcium gives physically consistent results, suggesting that the electrometer concept can be used to determine the cation binding affinity also to the lipid bilayers containing mixtures of PC and anionic lipids.

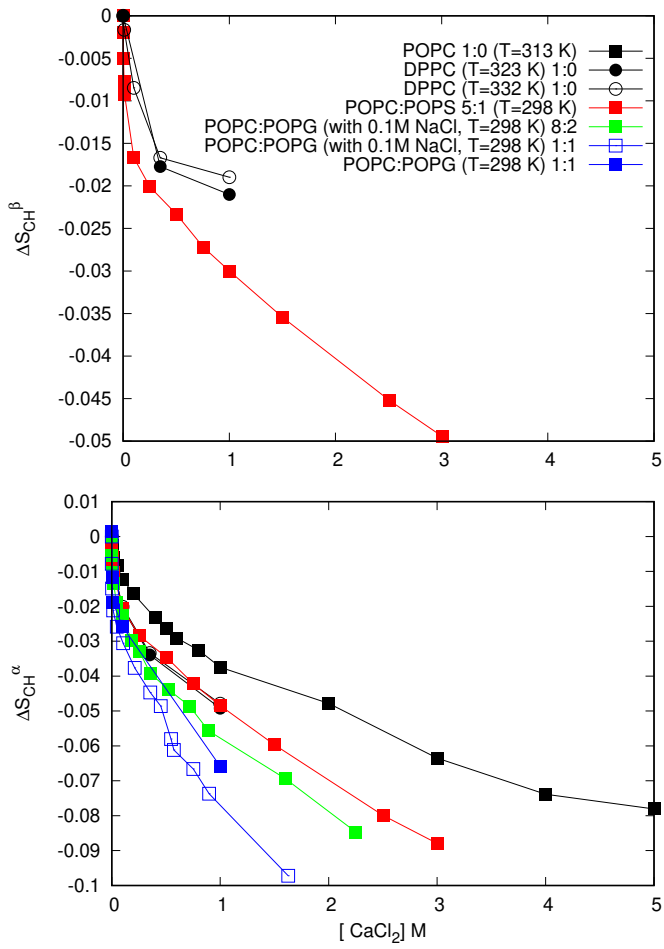


Figure S3: Changes of POPC headgroup order parameters as a function of CaCl_2 measured from mixed bilayers containing different amounts of anionic lipids. The original data is the same as in figure S2.

S3 Calibration of PC headgroup order parameter response to the bound cations

Before using the headgroup order parameters to compare ion binding affinity between simulations and experiments, the response of the order parameters to the bound charge in simulations should be quantified against experiments.^{90,91} In our previous work,⁹⁰ the ratio $\Delta S_{\text{CH}}^{\beta}/\Delta S_{\text{CH}}^{\alpha}$ was in good agreement with the experiments⁷⁸ in the Lipid14 model, but was underestimated by other models. In the more recent study,⁹¹ the headgroup order parameter responses were compared more carefully with the experiments of cationic dihexadecyldimethylammonium bromide (DHAB) surfactants in POPC bilayer.⁸¹ The comparison reveals that the both headgroup order parameters in the Lipid14 model are too sensitive to the bound charge, while CHARMM36 gives better agreement for the α carbon (Fig. S4). Therefore, the headgroup order parameter response to the bound charge is actually more realistic in CHARMM36 model than in the Lipid14. In the latter, both order parameters are equally too sensitive to the bound cations giving a good result for the $\Delta S_{\text{CH}}^{\beta}/\Delta S_{\text{CH}}^{\alpha}$ ratio. The ratio was overestimated for the CHARMM36 model because the β -carbon order parameter is relatively more sensitive than the α -carbon order parameter. These results have to be taken into account when analysing the ion binding affinities using headgroup order parameters in simulations. However, we conclude that the discrepancies arising from the sensitivity of lipid headgroup to bound charge are typically smaller than the discrepancies arising from ion binding affinity.

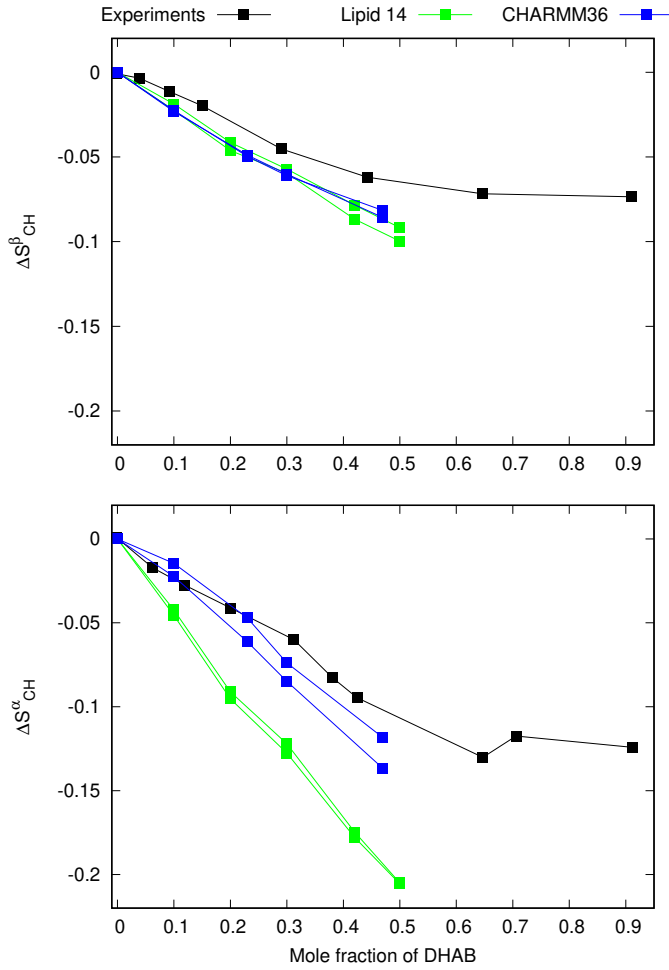


Figure S4: Responses of headgroup order parameters to the fixed amount of cationic surfactants in POPC bilayer from simulations and experiments.⁸¹ The simulation results for Lipid14 are directly from Ref. 91. The CHARMM36 simulation data and details are available from Ref. 92.

S4 Effect of the definition of concentration on the headgroup order parameters as a function of ion concentration.

Previous studies using the electrometer concept to assess the ion binding affinity to lipid bilayers report ion concentrations either in water before solvating the lipids (buffer concentration)^{1,78,90} or in bulk water after solvating the lipids (bulk concentration).^{79,91} In this work, we use the former definition to be consistent with the reference experimental data.¹ The difference between these two concentrations increases with the increasing ion binding affinity. However, the difference is essentially negligible in the recent model⁹¹ with realistic ion binding affinity (Fig. S5).

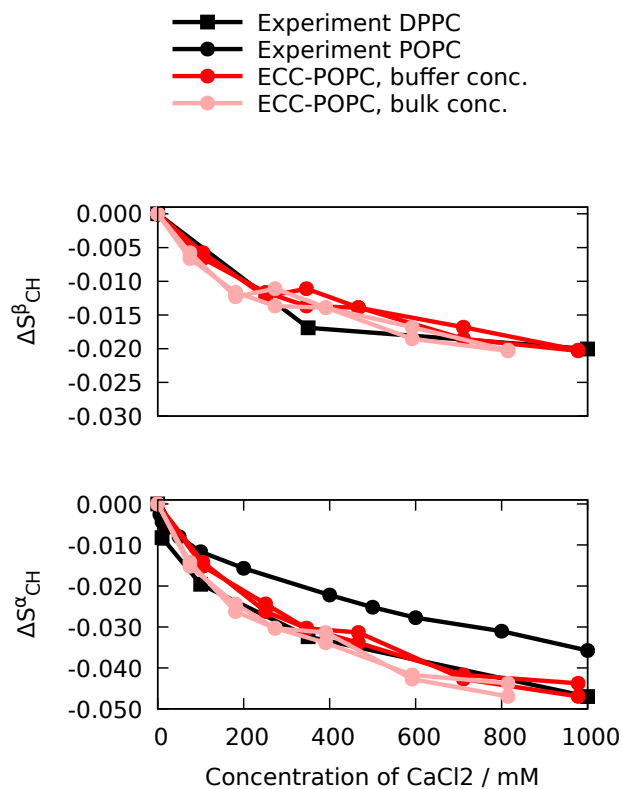


Figure S5: Changes of the headgroup order parameters as a function of CaCl_2 concentration using two possible definitions of ion concentration from the recent force field with realistic calcium binding affinity to a POPC bilayer⁹¹ together with the experimental data.^{78,79}

S5 Dipolar slices of the R-PDFL experiment

Slices of the R-PDFL spectra (Fig. S6) show a single splitting for the β -carbon with the order parameter value of 0.11, and a superposition of a large and a very small splitting for the α -carbon. The larger splitting from the α -carbon gives a order parameter value of 0.09, while the numerical value from the small splitting cannot resolved with the available resolution.

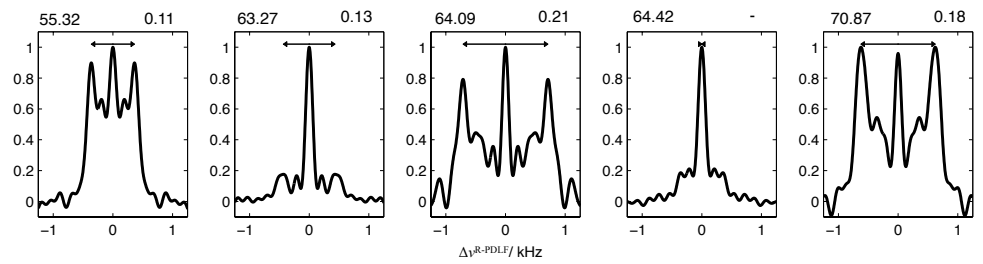


Figure S6: Dipolar coupling slices from the R-PDFL experiment.
Labeling of carbons and explanations of numbers (chemical shift and order parameter) would be good. The splitting corresponding the larger α -carbon order parameter should be also shown. Also, the size of the figure in the file may not be optimal.

S6 Dihedral angle distributions of the headgroup and glycerol backbone regions of PS lipids from different simulation models

The dihedral angles and structures of the glycerol backbone and headgroup regions of POPS lipids show wide variety between different simulation models (Figs. S7, S8 and S9). Detailed discussion of the structural differences is limited by the lack of realistic model that would correctly reproduce the headgroup and glycerol backbone order parameters. However, some structural characteristics of PS headgroup can be suggested based on the best available models (Figs. S10, S11 and S12), as discussed in the main text. The glycerol backbone structures are not discussed in this work because our focus is on PS headgroup. However, the data presented here can be useful for future investigations.

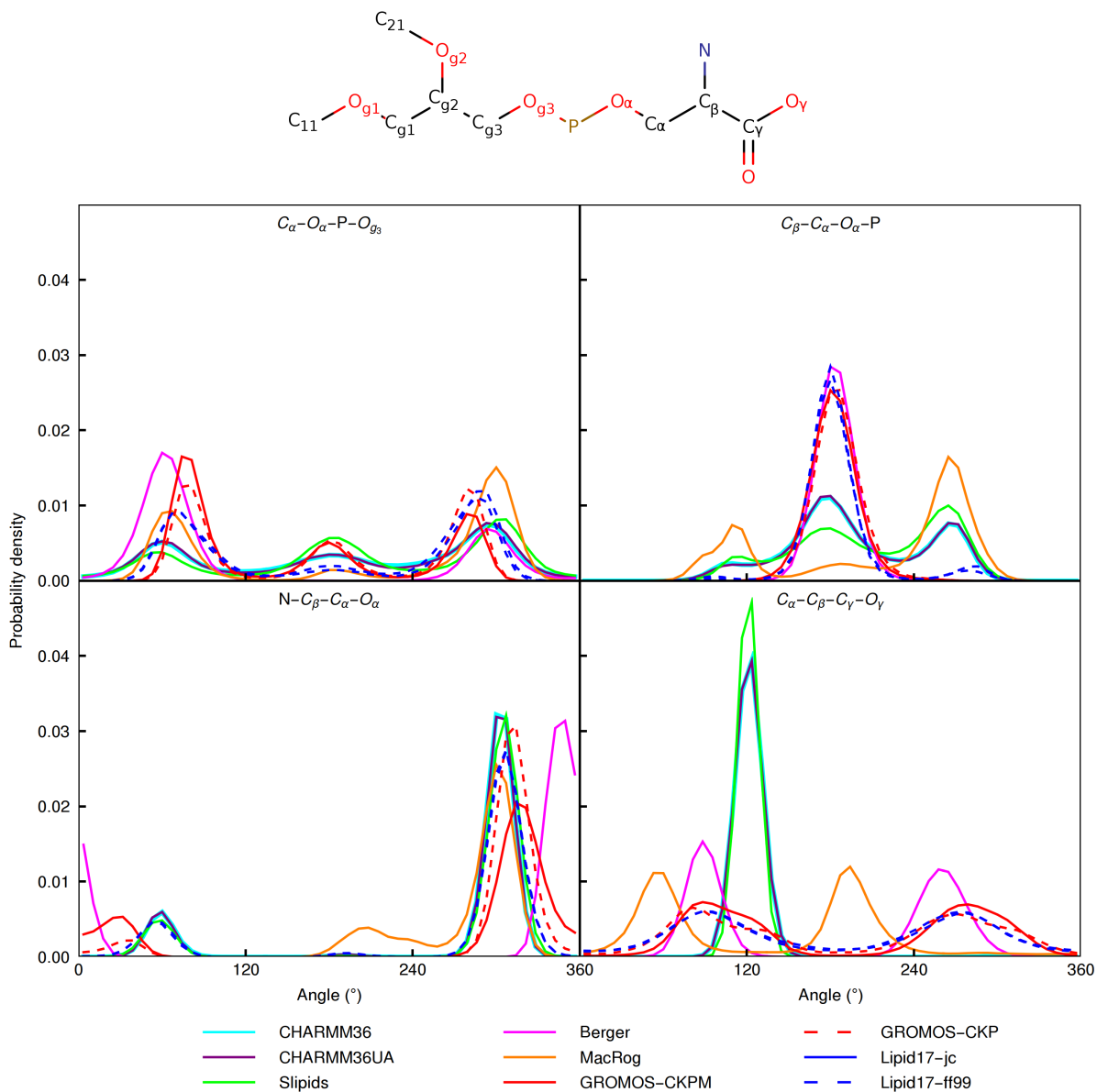


Figure S7: Dihedral angle distributions of the headgroup region of POPS from different simulation models.

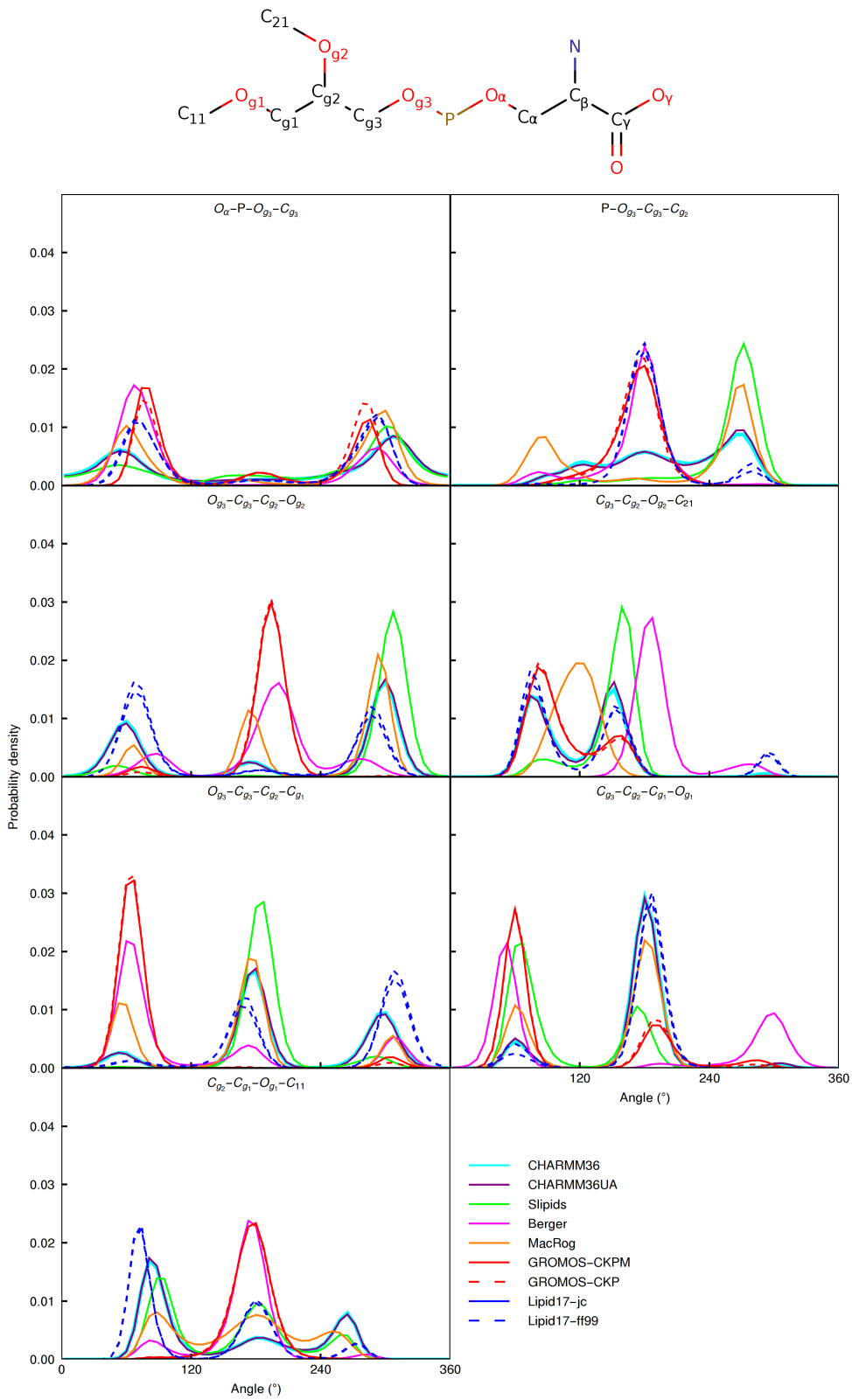


Figure S8: Dihedral angle distributions of the glycerol backbone region of POPS lipids from different simulation models.

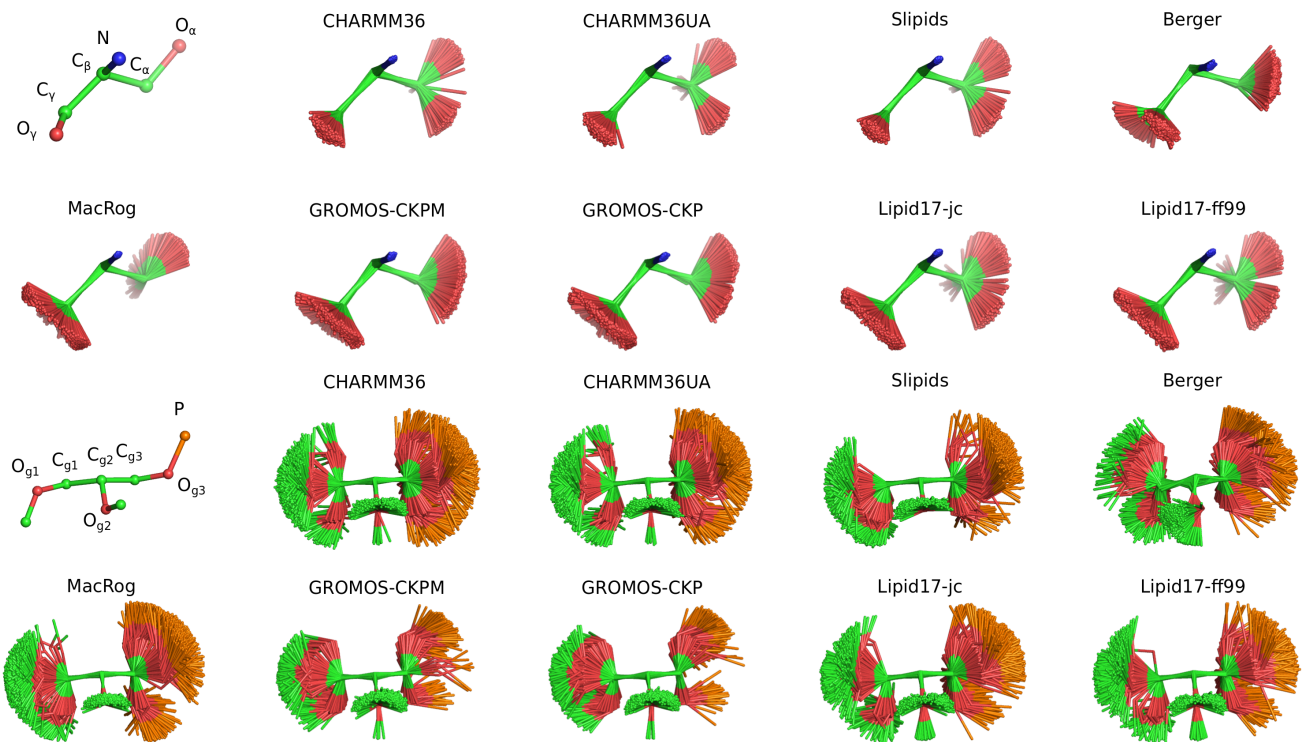


Figure S9: Overlayed snapshots of the glycerol backbone and headgroup regions from different POPS simulations.

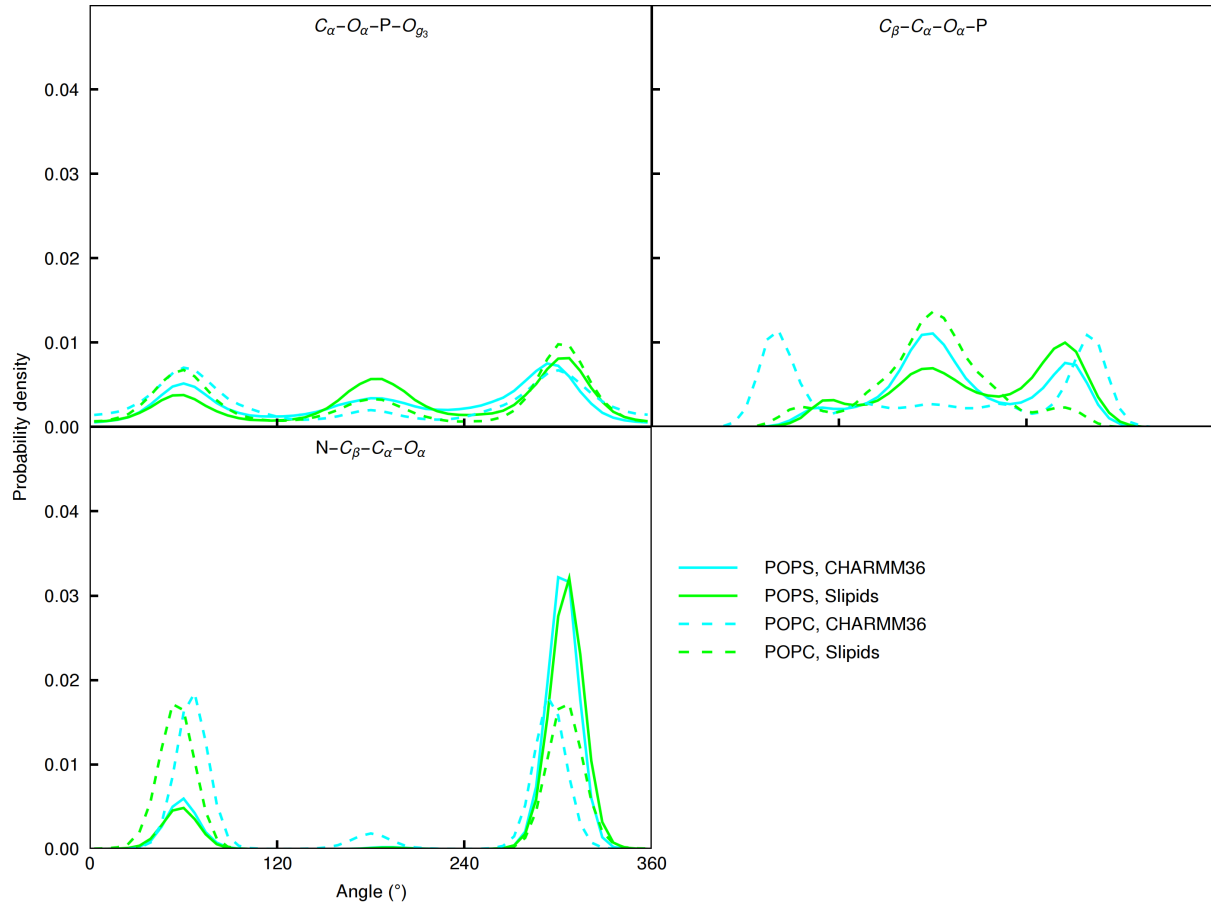


Figure S10: Dihedral angle distributions of the headgroup regions from CHARMM36 and Slipids simulations compared between the POPC and POPS lipids. The CHARMM36 POPC simulation is from Ref. 93 and Slipids POPC from Ref. 94.

Colours with more contrast would be better. The y-axis scale could be zoomed.

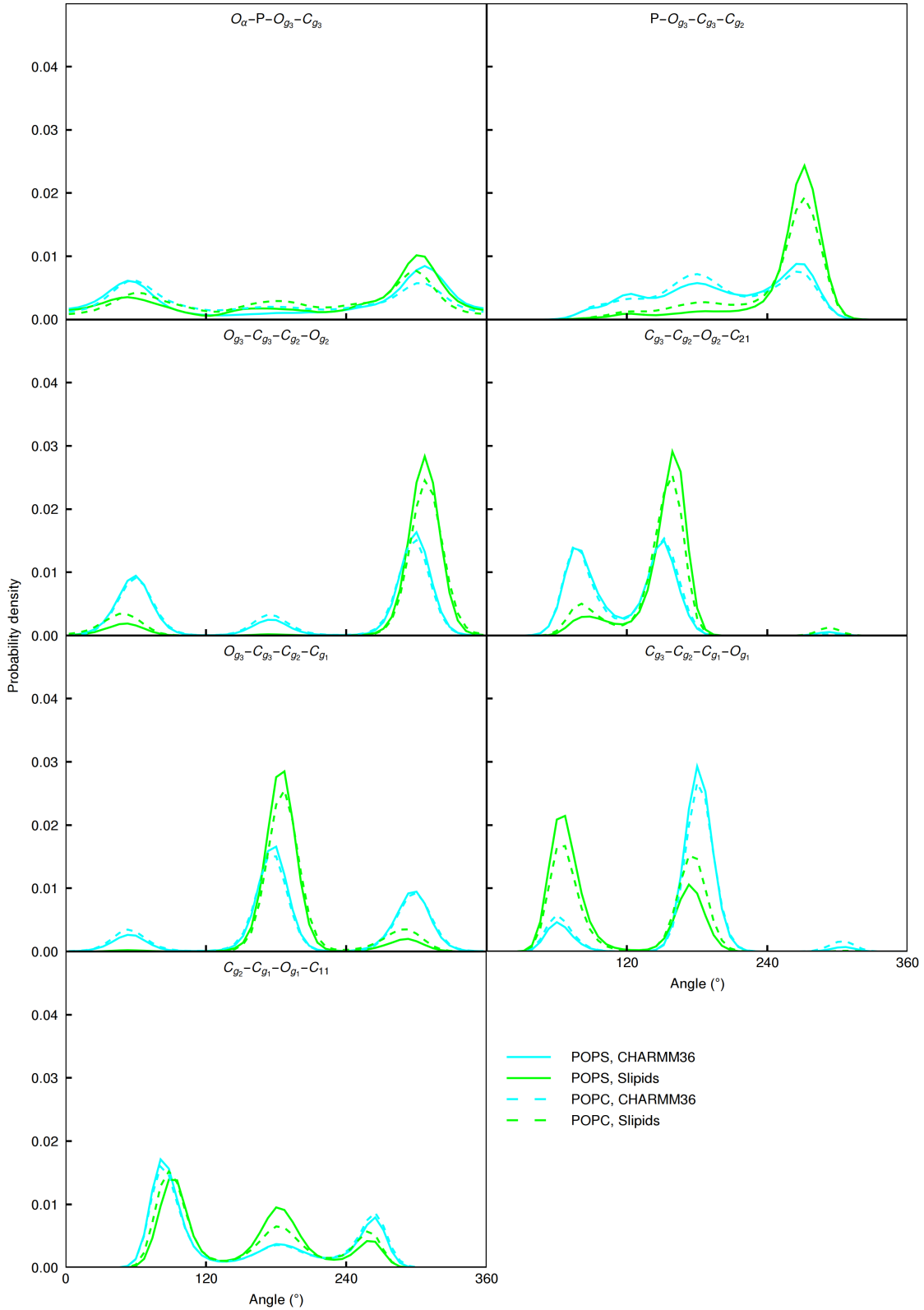


Figure S11: Dihedral angle distributions of the glycerol backbone regions from CHARMM36 and Slipids simulations compared between the POPC and POPS lipids. The CHARMM36 POPC simulation is from Ref. 93 and Slipids POPC from Ref. 94.

Colours with more contrast would be better. The y-axis scale could be zoomed.

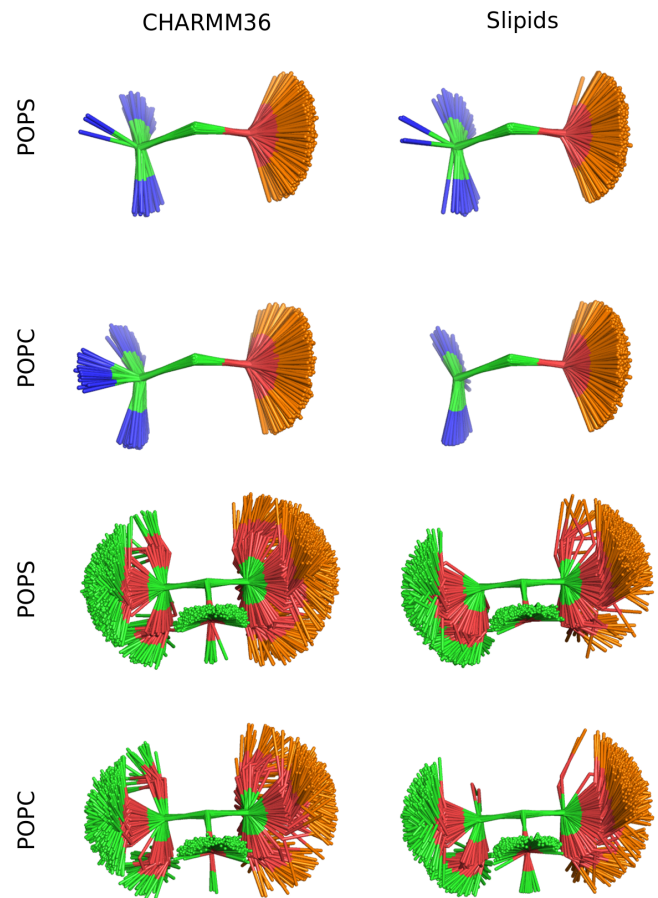


Figure S12: Overlayed snapshots of the headgroup and glycerol backbone regions from CHARMM36 and Slipids simulations compared between the POPC and POPS lipids. The CHARMM36 POPC simulation is from Ref. 93 and Slipids POPC from Ref. 94.

S7 Headgroup response to the additional counterions in POPC:POPS (5:1) mixtures

To evaluate counterion binding in different simulation models against experimental data,¹ we plot the headgroup order parameters measured from POPC:POPS 5:1 mixture as a function of different monovalent ions added to the buffer (Fig. S13). Experimental order parameters of POPC headgroup in the mixture are available as a function of LiCl and KCl concentrations, while POPS headgroup order parameters are measured also as a function of NaCl. Lithium interacts more strongly with PS headgroups than other monovalent ions,^{1,84,95–97} as also observed for PC headgroups.⁹⁸ The different binding behaviour is evident also in the changes of PS headgroup order parameters, which decrease with the addition of lithium but increase with the addition of sodium or potassium (Fig. S13). POPC headgroup order parameters exhibit a clear decrease as a function of LiCl concentration but only modest changes as a function of KCl concentration, indicating significant Li⁺ binding but only weak K⁺ binding to the mixture when interpreted using the electrometer concept.^{78–80}

In simulations with Berger and CHARMM36 models, the responses of headgroup order parameter of both POPC and POPS to the added sodium or potassium are more similar to the experiments with LiCl (Fig. S13), indicating overestimated binding affinity of sodium and potassium in these simulations. The MacRog simulations with potassium exhibit weaker counterion binding affinity (Fig. S14), but significantly larger error bars and less systematic changes in the order parameters (Fig. S13). Similar unsystematic behaviour was also observed in the simulations of Lipid14/17 model with the additional counterions,^{16–19} for which the data is not shown due to the formation of ion clusters in water with relatively low (1 M) ion concentrations (Fig. S15). Appearance of such clusters also in the MagRog simulations with 4 M concentration of KCl could explain the unsystematic changes of the order parameters in this model with the added KCl. In conclusion, the results are in line with the section 23 in the main text, suggesting that the MacRog simulations with KCl give the most realistic

surface charge at the lipid bilayer interface among the tested simulation models.

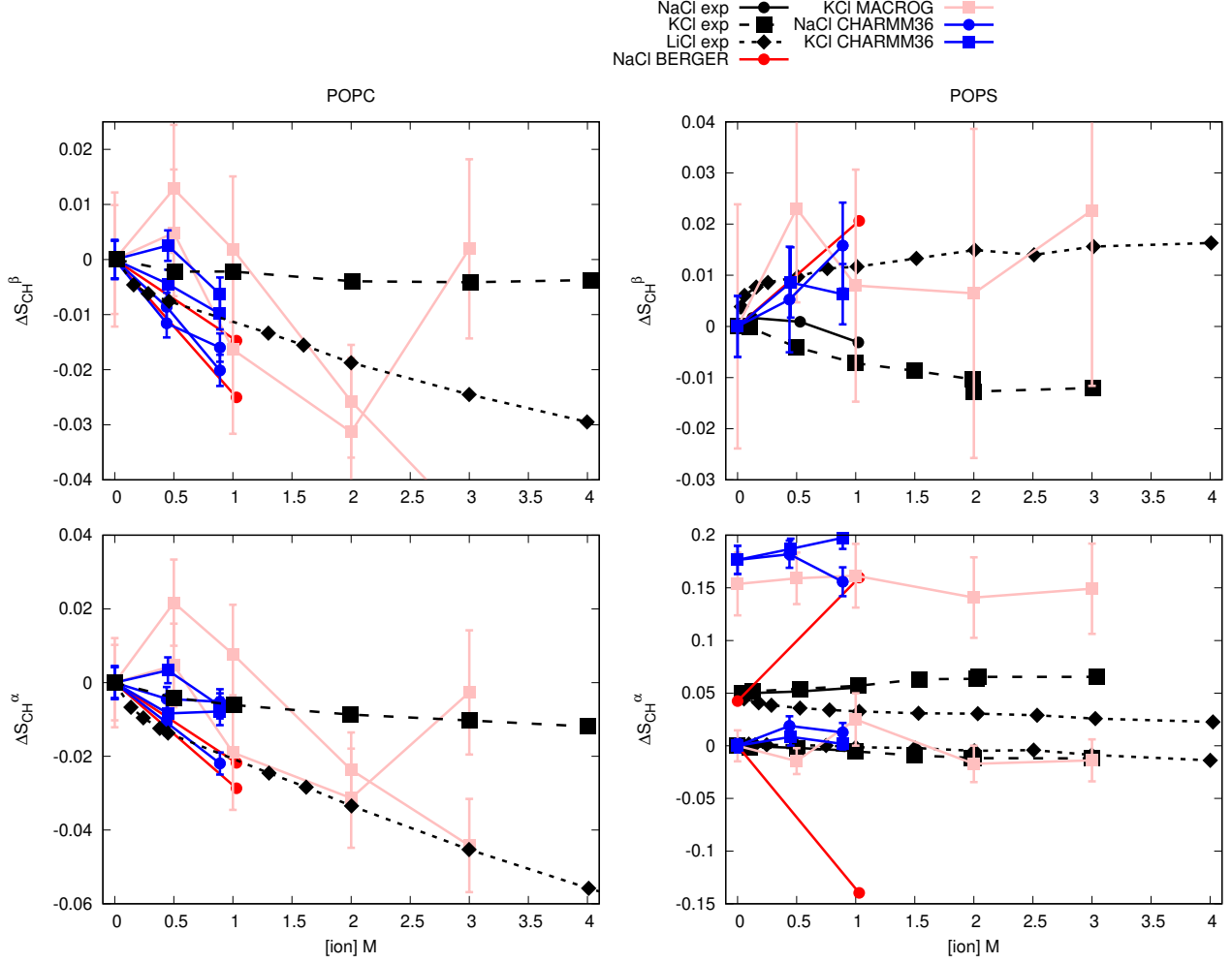


Figure S13: Changes of the PC (left) and PS (right) headgroup order parameters as a function of added NaCl, KCl and LiCl from POPC:POPS (5:1) mixture at 298 K (except Berger simulations are (4:1) mixture at 310 K). The experimental data is from Ref. 1. The values from counterion-only systems are set as a zero point of y-axis. To correctly illustrate the significant forking of the α -carbon order parameter in PS headgroup (bottom, right), the y-axis is transferred with the same value for both order parameters such that the lower order parameter value is at zero.

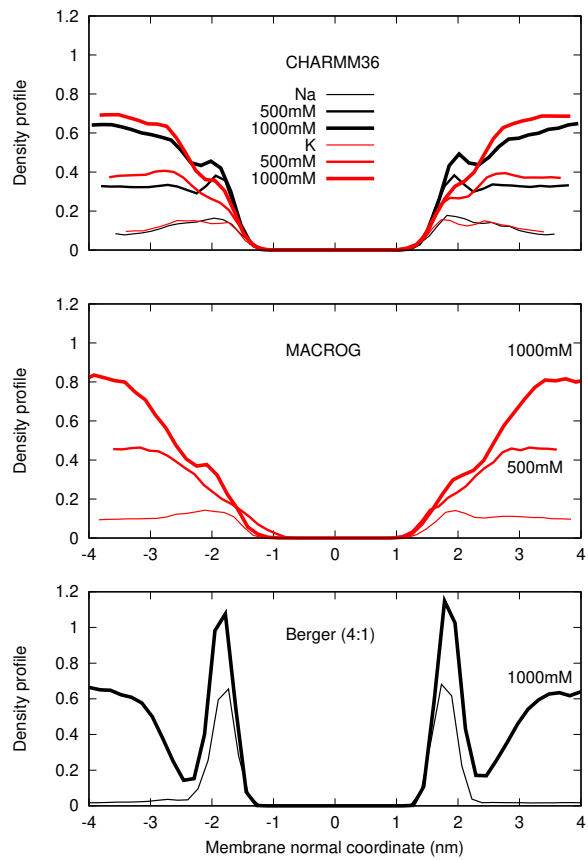


Figure S14: Counterion density distributions from PC:PS mixtures.

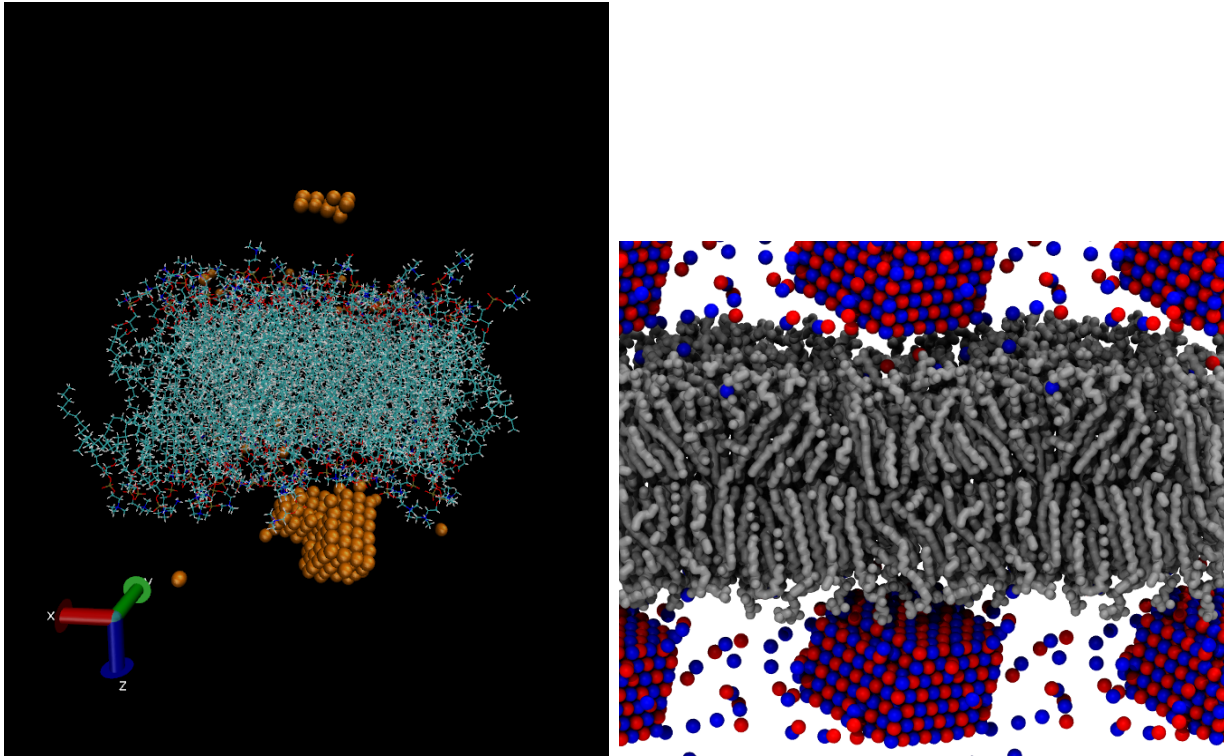


Figure S15: Ion clusters appearing in POPC:POPS (5:1) lipid17/14 simulations with 1 M of NaCl (left) and MacRog simulations with 4 M of KCl (right).

S8 Calcium binding to POPC in CHARMM36 simulation with NBfix

The response of POPC headgroup order parameters to the CaCl₂ concentration are underestimated in simulations of POPC:POPS (5:1) mixture with CHARMM36 containing the NBfix for interactions between calcium and lipid oxygens⁹⁹ (Fig. 9 in the main text), indicating that the calcium binding to the bilayer is too weak with these parameters. Without the NBfix term, the calcium binding affinity to pure POPC lipid bilayers was overestimated in the CHARMM36 model.⁹⁰ However, after employing the NBfix term, the response of headgroup order parameters (Fig. S16) and the binding affinity (Fig. S17) of calcium also to a pure POPC bilayer are underestimated. Notably, CHARMM36 simulations with the NBfix terms^{3,99} employed predict similar binding affinity for sodium and calcium. In conclusion, the special NBfix⁹⁹ for calcium, incorporated in the parameters give by the CHARMM-GUI at

the time of running the simulations (January 2018), leads to the underestimation of calcium binding affinity to pure PC and mixed PC:PS bilayers.

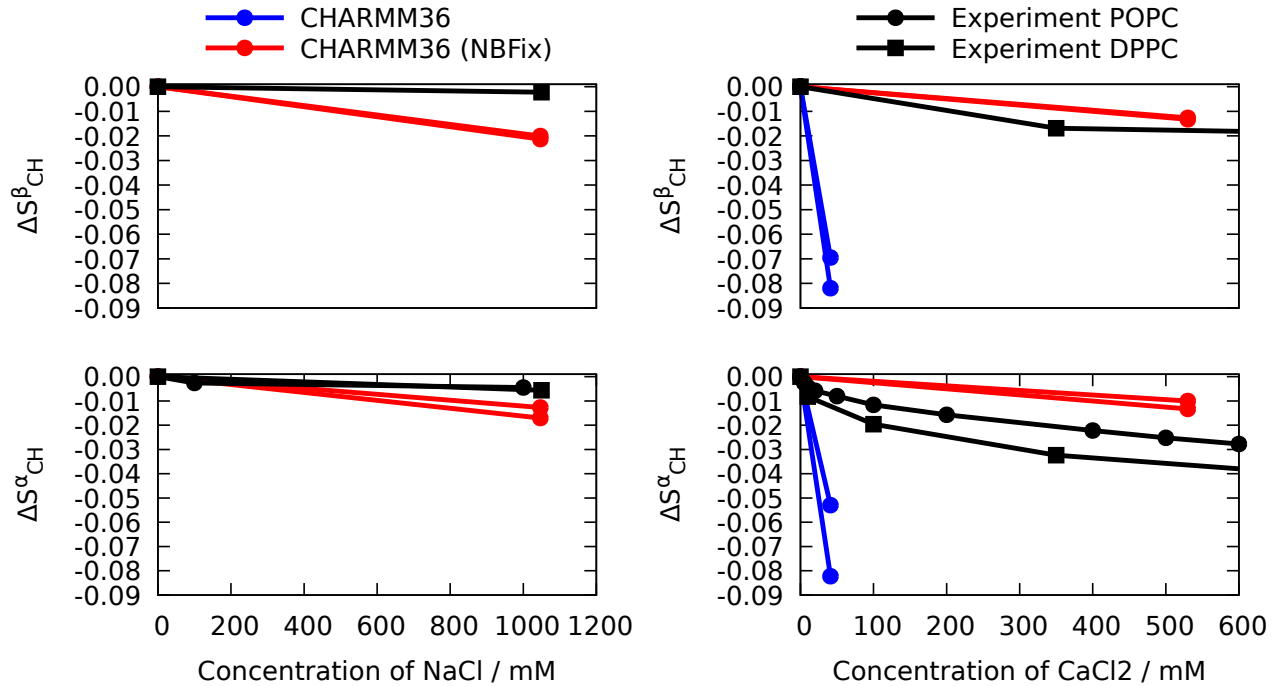


Figure S16: Headgroup order parameters from CHARMM36 simulations of POPC mixed with ions having the NBfix term employed for sodium³ (*left*) and calcium⁹⁹ (*right*) compared with the experimental data^{78,79} and simulations without NBfix for the calcium. Simulation files without ions are available at Ref. 100, with the NBfix term in sodium at Ref. 101, with the NBfix term in calcium at Ref. 101 and without the NBfix in calcium at Ref. 102.

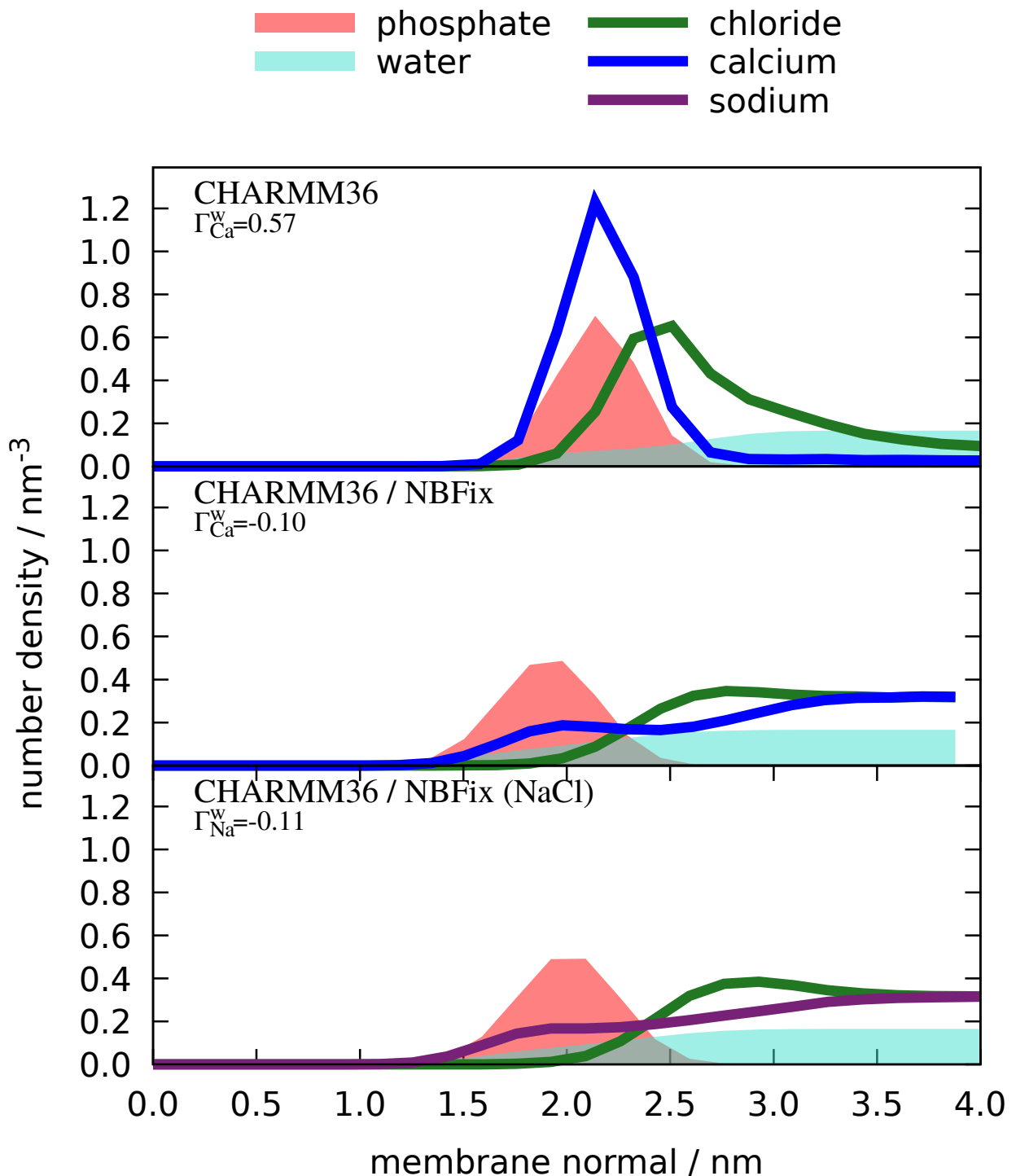


Figure S17: Density profiles along membrane normal from CHARMM36 simulations with (middle) and without (top) the NBfix term for calcium⁹⁹ compared to the simulation with the NBfix term for sodium³ (bottom). The simulation data are the same as in figure S16.

S9 Calcium density profiles from simulations with POPC:POPS(5:1) mixture

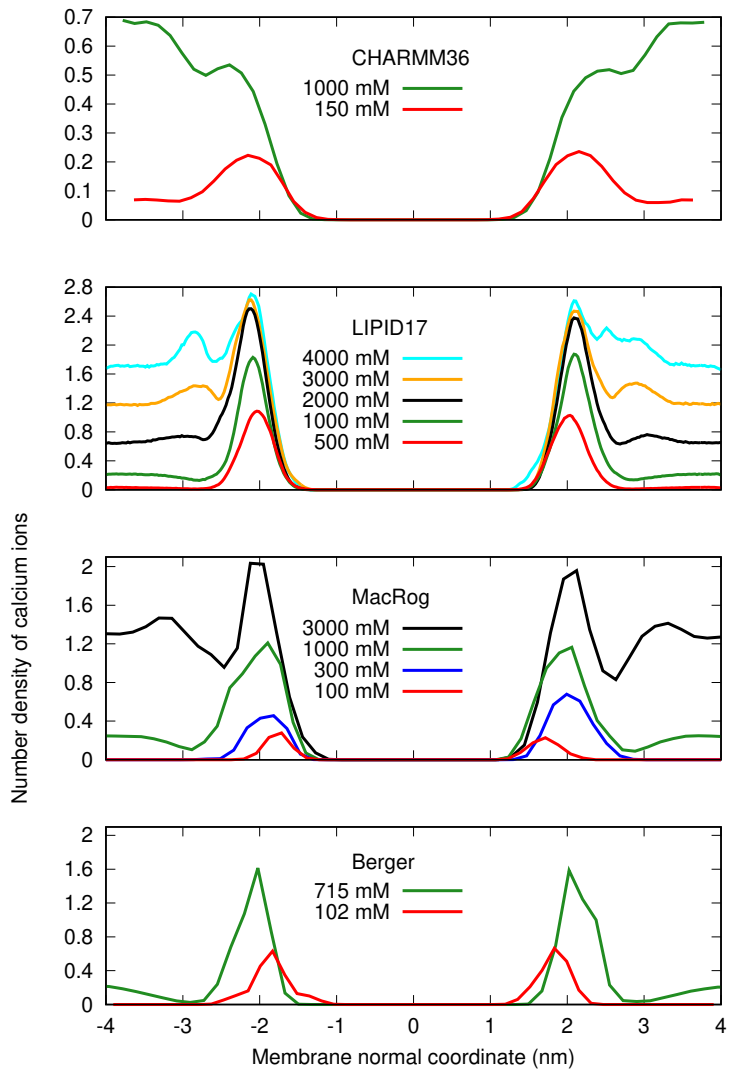


Figure S18: Ca^{2+} density profiles from simulations.
Should we include also counterions into the plot?

S10 Details of the rough subjective force field ranking (Fig. 5)

The assessment was based fully on the Fig. 3. First, for each carbon (the columns in Fig. 3) in each force field (the rows), we looked separately at deviations in magnitude and forking.

Magnitude deviations, i.e., how close to the experimentally obtained C–H order parameters (OPs) the force-field-produced OPs were. For each carbon, the following 5-step scale was used:

0 (): More than half of all the calculated OPs (that is, of all different hydrogens in all different lipids) were within the *subjective sweet spots* (SSP, blue-shaded areas in Fig. 3).

1 (M): All the calculated OPs were < 0.03 units away from the SSP.

2 (M): All the calculated OPs were < 0.05 units away from the SSP.

3 (M): All the calculated OPs were < 0.10 units away from the SSP.

4 (M): Some of the calculated OPs were > 0.10 units away from the SSP.

Forking deviations, i.e., how well the difference in order parameters of two hydrogens attached to a given carbon matched that obtained experimentally. Note that this is not relevant for β and g_2 , which have only one hydrogen. For the α carbon, for which a considerable forking of 0.105 is experimentally seen, the following 5-step scale was used:

0 (): The distance D between the dots (that mark the measurement-time-weighted averages in Fig. 3) was $0.08 < D < 0.13$ units for all the calculated OPs (that is, for all different lipids).

1 (F): $(0.06 < D < 0.08)$ OR $(0.13 < D < 0.15)$.

2 (F): $(0.04 < D < 0.06)$ OR $(0.15 < D < 0.17)$.

3 (F): $(0.02 < D < 0.04)$ OR $(0.17 < D < 0.19)$.

4 (F): $(D < 0.02)$ OR $(0.19 < D)$.

For the g_3 carbon, for which no forking is indicated by experiments, the following 5-step scale was used:

0 (): $D < 0.02$.

1 (f): $0.02 < D < 0.04$.

2 (F): $0.04 < D < 0.06$.

3 (F): $0.06 < D < 0.08$.

4 (F): $0.08 < D$.

For the g_1 carbon, for which a considerable forking of 0.13 is experimentally seen, the following 5-step scale was used:

0 (): $0.11 < D < 0.15$.

1 (f): $(0.09 < D < 0.11)$ OR $(0.15 < D < 0.17)$.

2 (F): $(0.07 < D < 0.09)$ OR $(0.17 < D < 0.19)$.

3 (F): $(0.05 < D < 0.07)$ OR $(0.19 < D < 0.21)$.

4 (F): $(D < 0.05)$ OR $(0.21 < D)$.

Based on these assessments of magnitude and forking deviations, each carbon was then assigned to one of the following groups: "within experimental error" (magnitude and forking deviations both on step 0 of the scales described above), "almost within experimental error" (sum of the magnitude and forking deviation steps 1 or 2), "clear deviation from experiments" (sum of magnitude and forking deviation steps from 3 to 5), and "major deviation from experiments" (sum of magnitude and forking deviation steps from 6 to 8). These groups are

indicated by colors in Fig. 4. (Note that for β and g_2 , for which there can be no forking, the corresponding group assignment limits were: 0, 1, 2, and 3.)

Finally, the total ability of the force field to describe the headgroup and glycerol structure was estimated. To this end, the groups were given the following weights: 0 (within experimental error), 1 (almost within experimental error), 2 (clear deviation from experiments), 4 (major deviation from experiments), and the weights of the five carbons were summed up. The sum, given in the Σ -column of Fig. 3, was then used to (roughly and subjectively, as should be clear from the above description) rank the force fields.

References

- (1) Roux, M.; Bloom, M. Calcium, magnesium, lithium, sodium, and potassium distributions in the headgroup region of binary membranes of phosphatidylcholine and phosphatidylserine as seen by deuterium NMR. *Biochemistry* **1990**, *29*, 7077–7089.
- (2) Klauda, J. B.; Venable, R. M.; Freites, J. A.; O'Connor, J. W.; Tobias, D. J.; Mondragon-Ramirez, C.; Vorobyov, I.; MacKerell Jr, A. D.; Pastor, R. W. Update of the CHARMM All-Atom Additive Force Field for Lipids: Validation on Six Lipid Types. *J. Phys. Chem. B* **2010**, *114*, 7830–7843.
- (3) Venable, R. M.; Luo, Y.; Gawrisch, K.; Roux, B.; Pastor, R. W. Simulations of Anionic Lipid Membranes: Development of Interaction-Specific Ion Parameters and Validation Using NMR Data. *The Journal of Physical Chemistry B* **2013**, *117*, 10183–10192.
- (4) Madsen, J. J. MD simulations of bilayers containing PC/PS mixtures and CaCl₂:150POPC_150POPS_neutral. 2019; <https://doi.org/10.5281/zenodo.2542164>.
- (5) Piggot, T. CHARMM36 POPS/POPC simulations (versions 1 and 2) 298 K 1.0 nm LJ switching with K ions. 2018; <https://doi.org/10.5281/zenodo.1182658>.
- (6) Ollila, O. H. S. POPC:POPS (5:1) with 450 mM potassium simulation with CHARMM36 at 298K. 2018; <https://doi.org/10.5281/zenodo.1493241>.
- (7) Ollila, O. H. S. POPC:POPS (5:1) with 890 mM potassium simulation with CHARMM36 at 298K. 2018; <https://doi.org/10.5281/zenodo.1493246>.
- (8) Piggot, T. CHARMM36 POPS/POPC simulations (versions 1 and 2) 298 K 1.0 nm LJ switching with Na ions. 2018; <https://doi.org/10.5281/zenodo.1182665>.
- (9) Ollila, O. H. S. POPC:POPS (5:1) with 440 mM sodium simulation with CHARMM36 at 298K. 2018; <https://doi.org/10.5281/zenodo.1493190>.

- (10) Ollila, O. H. S. POPC:POPS (5:1) with 890 mM sodium simulation with CHARMM36 at 298K. 2018; <https://doi.org/10.5281/zenodo.1493229>.
- (11) Maciejewski, A.; Pasenkiewicz-Gierula, M.; Cramariuc, O.; Vattulainen, I.; Rög, T. Refined OPLS All-Atom Force Field for Saturated Phosphatidylcholine Bilayers at Full Hydration. *J. Phys. Chem. B* **2014**, *118*, 4571–4581.
- (12) Javanainen, M. Simulations of POPC/POPS membranes with CaCl₂. 2017; <https://doi.org/10.5281/zenodo.1409551>.
- (13) Javanainen, M. Simulations of POPC/POPS membranes with KCl. 2018; <https://doi.org/10.5281/zenodo.1404040>.
- (14) Dickson, C. J.; Madej, B. D.; Skjevik, A. A.; Betz, R. M.; Teigen, K.; Gould, I. R.; Walker, R. C. Lipid14: The Amber Lipid Force Field. *J. Chem. Theory Comput.* **2014**, *10*, 865–879.
- (15) Gould, I.; Skjevik, A.; Dickson, C.; Madej, B.; Walker, R. Lipid17: A Comprehensive AMBER Force Field for the Simulation of Zwitterionic and Anionic Lipids. 2018; In preparation.
- (16) Kav, B.; Miettinen, M. S. Amber Lipid17 Simulations of POPC/POPS Membranes with KCl Counterions. 2018; <https://doi.org/10.5281/zenodo.1250969>, B.K acknowledges financial support from International Max Planck Research School on Multiscale Bio-Systems.
- (17) Kav, B.; Miettinen, M. S. Amber Lipid17 Simulations of POPC/POPS Membranes with KCl. 2018; <https://doi.org/10.5281/zenodo.1227257>, B.K acknowledges financial support from International Max Planck Research School on Multiscale Bio-Systems.
- (18) Kav, B.; Miettinen, M. S. Amber Lipid17 Simulations of POPC/POPS Membranes with NaCl Counterions. 2018; <https://doi.org/10.5281/zenodo.1250975>, B.K acknowl-

edges financial support from International Max Planck Research School on Multiscale Bio-Systems.

- (19) Kav, B.; Miettinen, M. S. Amber Lipid17 Simulations of POPC/POPS Membranes with NaCl. 2018; <https://doi.org/10.5281/zenodo.1227272>, B.K acknowledges financial support from International Max Planck Research School on Multiscale Bio-Systems.
- (20) Tielemans, D. P.; Berendsen, H. J.; Sansom, M. S. An Alamethicin Channel in a Lipid Bilayer: Molecular Dynamics Simulations. *Biophys. J.* **1999**, *76*, 1757 – 1769.
- (21) Mukhopadhyay, P.; Monticelli, L.; Tielemans, D. P. Molecular Dynamics Simulation of a Palmitoyl-Oleoyl Phosphatidylserine Bilayer with Na⁺ Counterions and NaCl. *Biophysical Journal* **2004**, *86*, 1601 – 1609.
- (22) Samuli, O. O. H. POPC:POPS (4:1) simulation with Berger model at 310K. 2018; <https://doi.org/10.5281/zenodo.1475285>.
- (23) Cwiklik, L. MD simulation trajectory of a POPC/POPS (4:1) bilayer with 1M NaCl, Berger force field for lipids and ffgmx for ions. 2017; <https://doi.org/10.5281/zenodo.838219>.
- (24) Botan, A.; Favela-Rosales, F.; Fuchs, P. F. J.; Javanainen, M.; Kanduč, M.; Kulig, W.; Lamberg, A.; Loison, C.; Lyubartsev, A.; Miettinen, M. S. et al. Toward Atomistic Resolution Structure of Phosphatidylcholine Headgroup and Glycerol Backbone at Different Ambient Conditions. *J. Phys. Chem. B* **2015**, *119*, 15075–15088.
- (25) Fernando, F.-R. POPC_Glycerol_CHARMM36_0-10-15-20-25-35-50%CHOL. 2015; <http://dx.doi.org/10.5281/zenodo.16830>, Because of the system size, the files ONLY contain the coordinates of Glycerol saved every 10ps, this is the real contribution to the nmrlipids project.

- (26) Piggot, T. CHARMM36 DOPS simulations (versions 1 and 2) 303 K 1.0 nm LJ switching. 2017; <https://doi.org/10.5281/zenodo.1129411>.
- (27) Piggot, T. CHARMM36 POPS simulations (versions 1 and 2) 298 K 1.0 nm LJ switching. 2017; <https://doi.org/10.5281/zenodo.1129415>.
- (28) Piggot, T. CHARMM36 POPS simulations (versions 1 and 2) 298 K 1.0 nm LJ switching with K ions. 2018; <https://doi.org/10.5281/zenodo.1182654>.
- (29) Madsen, J. J. MD simulations of bilayers containing PC/PS mixtures and CaCl₂: 250POPC_50POPS_neutral. 2019; <https://doi.org/10.5281/zenodo.2542151>.
- (30) Lee, J.; Cheng, X.; Swails, J. M.; Yeom, M. S.; Eastman, P. K.; Lemkul, J. A.; Wei, S.; Buckner, J.; Jeong, J. C.; Qi, Y. et al. CHARMM-GUI Input Generator for NAMD, GROMACS, AMBER, OpenMM, and CHARMM/OpenMM Simulations Using the CHARMM36 Additive Force Field. *Journal of Chemical Theory and Computation* **2016**, *12*, 405–413.
- (31) Jo, S.; Kim, T.; Iyer, V. G.; Im, W. CHARMM-GUI: A web-based graphical user interface for CHARMM. *Journal of Computational Chemistry* **29**, 1859–1865.
- (32) Abraham, M. J.; Murtola, T.; Schulz, R.; Páll, S.; Smith, J. C.; Hess, B.; Lindahl, E. GROMACS: High performance molecular simulations through multi-level parallelism from laptops to supercomputers. *SoftwareX* **2015**, *1*, 19–25.
- (33) Madsen, J. J. MD simulations of bilayers containing PC/PS mixtures and CaCl₂: 250POPC_50POPS_0.15M_{CaCl}₂. 2019; <https://doi.org/10.5281/zenodo.2542176>.
- (34) Madsen, J. J. MD simulations of bilayers containing PC/PS mixtures and CaCl₂: 250POPC_50POPS_1M_{CaCl}₂. 2019; <https://doi.org/10.5281/zenodo.2542135>.

- (35) Piggot, T. CHARMM36-UA DOPS simulations (versions 1 and 2) 303 K 1.0 nm LJ switching. 2017; <https://doi.org/10.5281/zenodo.1129456>.
- (36) Piggot, T. CHARMM36-UA POPS simulations (versions 1 and 2) 298 K 1.0 nm LJ switching. 2017; <https://doi.org/10.5281/zenodo.1129458>.
- (37) Kulig, W.; Pasenkiewicz-Gierula, M.; RÅsg, T. Topologies, structures and parameter files for lipid simulations in GROMACS with the OPLS-aa force field: DPPC, POPC, DOPC, PEPC, and cholesterol. *Data in Brief* **2015**, *5*, 333 – 336.
- (38) Kulig, W.; Pasenkiewicz-Gierula, M.; R  g, T. Cis and trans unsaturated phosphatidyl-choline bilayers: A molecular dynamics simulation study. *Chem. Phys. Lipids* **2016**, *195*, 12 – 20.
- (39) Jorgensen, W. L.; Chandrasekhar, J.; Madura, J. D.; Impey, R. W.; Klein, M. L. Comparison of simple potential functions for simulating liquid water. *J. Chem. Phys.* **1983**, *79*, 926–935.
- (40) Javanainen, M. Simulation of a POPC bilayer at 298K, lipid model by Maciejewski and Rog. 2018; <https://doi.org/10.5281/zenodo.1167532>.
- (41) Piggot, T. MacRog POPS simulations (versions 1 and 2) 298 K with corrected PO not OP tails. 2018; <https://doi.org/10.5281/zenodo.1283335>.
- (42) Javanainen, M. Simulation of a POPS membrane with potassium counterions. 2018; <https://doi.org/10.5281/zenodo.1434990>.
- (43) Åqvist, J. Ion-water interaction potentials derived from free energy perturbation simulations. *J. Phys. Chem.* **1990**, *94*, 8021–8024.
- (44) RÅsg, T.; OrÅ owski, A.; Llorente, A.; Skotland, T.; Sylv  nne, T.; Kauhanen, D.; Ekroos, K.; Sandvig, K.; Vattulainen, I. Data including GROMACS input files for atomistic molecular dynamics simulations of mixed, asymmetric bilayers including

molecular topologies, equilibrated structures, and force field for lipids compatible with OPLS-AA parameters. *Data in Brief* **2016**, *7*, 1171 – 1174.

- (45) Essman, U. L.; Perera, M. L.; Berkowitz, M. L.; Larden, T.; Lee, H.; Pedersen, L. G. A smooth particle mesh ewald potential. *J. Chem. Phys.* **1995**, *103*, 8577–8592.
- (46) Shirts, M. R.; Mobley, D. L.; Chodera, J. D.; Pande, V. S. Accurate and Efficient Corrections for Missing Dispersion Interactions in Molecular Simulations. *The Journal of Physical Chemistry B* **2007**, *111*, 13052–13063.
- (47) Nose, S. A molecular dynamics method for simulations in the canonical ensemble. *Mol. Phys.* **1984**, *52*, 255–268.
- (48) Hoover, W. G. Canonical dynamics: Equilibrium phase-space distributions. *Phys. Rev. A* **1985**, *31*, 1695–1697.
- (49) Parrinello, M.; Rahman, A. Polymorphic transitions in single crystals: A new molecular dynamics method. *J. Appl. Phys.* **1981**, *52*, 7182–7190.
- (50) Hess, B.; Bekker, H.; Berendsen, H. J. C.; Fraaije, J. G. E. M. LINCS: a linear constraint solver for molecular dynamics simulations. *J. Comput. Chem.* **1997**, *18*, 1463–1472.
- (51) Hess, B. P-LINCS: A Parallel Linear Constraint Solver for Molecular Simulation. *J. Chem. Theory Comput.* **2008**, *4*, 116–122.
- (52) Miyamoto, S.; Kollman, P. A. SETTLE: An analytical Version of the SHAKE and RATTLE Algorithm for Rigid Water Models. *J. Comput. Chem.* **1992**, *13*, 952–962.
- (53) Jorgensen, W. L.; Chandrasekhar, J.; Madura, J. D.; Impey, R. W.; Klein, M. L. Comparison of simple potential functions for simulating liquid water. *The Journal of chemical physics* **1983**, *79*, 926–935.

- (54) Joung, I. S.; Cheatham III, T. E. Determination of alkali and halide monovalent ion parameters for use in explicitly solvated biomolecular simulations. *The journal of physical chemistry B* **2008**, *112*, 9020–9041.
- (55) Miettinen, M. S.; Kav, B. Molecular dynamics simulation trajectory of an anionic lipid bilayer: 100 mol% POPS with Na⁺ counterions using Joung-Cheatham Ions. 2018; <https://doi.org/10.5281/zenodo.1148495>, B.K. acknowledges financial support from International Max Planck Research School on Multiscale Bio-Systems.
- (56) Miettinen, M. S.; Kav, B. Molecular dynamics simulation trajectory of an anionic lipid bilayer: 100 mol% POPS with Na⁺ counterions using ff99 ions. 2018; <https://doi.org/10.5281/zenodo.1134869>, B.K. acknowledges financial support from International Max Planck Research School on Multiscale Bio-Systems.
- (57) Kav, B.; Miettinen, M. S. Molecular dynamics simulation trajectory of an anionic lipid bilayer: 100 mol% DOPS with Na⁺ counterions using Joung-Cheetham Ions. 2018; <https://doi.org/10.5281/zenodo.1134871>, B.K acknowledges financial support from International Max Planck Research School on Multiscale Bio-Systems.
- (58) Kav, B.; Miettinen, M. S. Molecular dynamics simulation trajectory of an anionic lipid bilayer: 100 mol% DOPS with Na⁺ counterions using ff99 Ions. 2018; <https://doi.org/10.5281/zenodo.1135142>, B.K acknowledges financial support from International Max Planck Research School on Multiscale Bio-Systems.
- (59) Melcr, J. Molecular dynamics simulations of lipid bilayers containing POPC and POPS with the lipid17 force field, only counterions, and CaCl₂ concentrations. 2018; <https://doi.org/10.5281/zenodo.1487761>.
- (60) Kav, B.; Miettinen, M. S. Amber Lipid17 Simulations of POPC/POPS Membranes with CaCl₂. 2018; <https://doi.org/10.5281/zenodo.1438848>, B.K acknowledges

financial support from International Max Planck Research School on Multiscale Bio-Systems.

- (61) Ollila, S.; Hyvönen, M. T.; Vattulainen, I. Polyunsaturation in Lipid Membranes: Dynamic Properties and Lateral Pressure Profiles. *J. Phys. Chem. B* **2007**, *111*, 3139–3150.
- (62) Ollila, O. H. S. MD simulation of POPC lipids bilayer at 310K (Berger, Gromacs 3.1.4). 2018; <https://doi.org/10.5281/zenodo.1230170>.
- (63) Piggot, T. Berger POPS simulations (versions 1 and 2) 298 K 1.0 nm cut-off. 2017; <https://doi.org/10.5281/zenodo.1129425>.
- (64) Piggot, T. Berger DOPS simulations (versions 1 and 2) 303 K 1.0 nm cut-off. 2017; <https://doi.org/10.5281/zenodo.1129419>.
- (65) Jurkiewicz, P.; Cwiklik, L.; Vojtěchová, A.; Jungwirth, P.; Hof, M. Structure, dynamics, and hydration of POPC/POPS bilayers suspended in NaCl, KCl, and CsCl solutions. *Biochimica et Biophysica Acta (BBA) - Biomembranes* **2012**, *1818*, 609 – 616.
- (66) Melcrová, A.; Pokorna, S.; Pullanchery, S.; Kohagen, M.; Jurkiewicz, P.; Hof, M.; Jungwirth, P.; Cremer, P. S.; Cwiklik, L. The complex nature of calcium cation interactions with phospholipid bilayers. *Sci. Reports* **2016**, *6*, 38035.
- (67) Lukasz, C. MD simulation trajectory of a POPC/POPS (4:1) bilayer with 102mM CaCl₂, Berger force field for lipids, scaled charges for Ca²⁺ and Cl⁻. 2017; <https://doi.org/10.5281/zenodo.887398>.
- (68) Lukasz, C. MD simulation trajectory of a POPC/POPS (4:1) bilayer with 715mM CaCl₂, Berger force field for lipids, scaled charges for Ca²⁺ and Cl⁻. 2017; <https://doi.org/10.5281/zenodo.887400>.

- (69) Piggot, T. GROMOS-CKP POPS simulations (versions 1 and 2) 298 K with Berger/Chiu NH3 charges and PME. 2017; <https://doi.org/10.5281/zenodo.1129431>.
- (70) Piggot, T. GROMOS-CKP POPS simulations (versions 1 and 2) 298 K with GROMOS NH3 charges and PME. 2017; <https://doi.org/10.5281/zenodo.1129435>.
- (71) Piggot, T. GROMOS-CKP DOPS simulations (versions 1 and 2) 303 K with Berger/Chiu NH3 charges and PME. 2017; <https://doi.org/10.5281/zenodo.1129429>.
- (72) Piggot, T. GROMOS-CKP DOPS simulations (versions 1 and 2) 303 K with GROMOS NH3 charges and PME. 2017; <https://doi.org/10.5281/zenodo.1129447>.
- (73) Piggot, T. GROMOS-CKP POPS/POPC simulations (versions 1 and 2) 298 K with GROMOS NH3 charges and PME. 2018; <https://doi.org/10.5281/zenodo.1283333>.
- (74) Piggot, T. GROMOS-CKP POPS/POPC simulations (versions 1 and 2) 298 K with Berger/Chiu NH3 charges and PME. 2018; <https://doi.org/10.5281/zenodo.1283331>.
- (75) Piggot, T. Slipids POPS simulations (versions 1 and 2) 298 K 1.0 nm cut-off with LJ-PME. 2017; <https://doi.org/10.5281/zenodo.1129441>.
- (76) Piggot, T. Slipids DOPS simulations (versions 1 and 2) 303 K 1.0 nm cut-off with LJ-PME. 2017; <https://doi.org/10.5281/zenodo.1129439>.
- (77) Favela-Rosales, F. MD simulation trajectory of a fully hydrated DOPS bilayer: SLIPIDS, Gromacs 5.0.4. 2017. 2017; <https://doi.org/10.5281/zenodo.495510>.
- (78) Akutsu, H.; Seelig, J. Interaction of metal ions with phosphatidylcholine bilayer membranes. *Biochemistry* **1981**, *20*, 7366–7373.

- (79) Altenbach, C.; Seelig, J. Calcium binding to phosphatidylcholine bilayers as studied by deuterium magnetic resonance. Evidence for the formation of a calcium complex with two phospholipid molecules. *Biochemistry* **1984**, *23*, 3913–3920.
- (80) Seelig, J.; MacDonald, P. M.; Scherer, P. G. Phospholipid head groups as sensors of electric charge in membranes. *Biochemistry* **1987**, *26*, 7535–7541.
- (81) Scherer, P. G.; Seelig, J. Electric charge effects on phospholipid headgroups. Phosphatidylcholine in mixtures with cationic and anionic amphiphiles. *Biochemistry* **1989**, *28*, 7720–7728.
- (82) Borle, F.; Seelig, J. Ca²⁺ binding to phosphatidylglycerol bilayers as studied by differential scanning calorimetry and ²H- and ³¹P-nuclear magnetic resonance. *Chemistry and Physics of Lipids* **1985**, *36*, 263 – 283.
- (83) Macdonald, P. M.; Seelig, J. Calcium binding to mixed phosphatidylglycerol-phosphatidylcholine bilayers as studied by deuterium nuclear magnetic resonance. *Biochemistry* **1987**, *26*, 1231–1240.
- (84) Roux, M.; Neumann, J.-M. Deuterium NMR study of head-group deuterated phosphatidylserine in pure and binary phospholipid bilayers. *FEBS Letters* **1986**, *199*, 33–38.
- (85) Roux, M.; Bloom, M. Calcium binding by phosphatidylserine headgroups. Deuterium NMR study. *Biophys. J.* **1991**, *60*, 38 – 44.
- (86) Scherer, P.; Seelig, J. Structure and dynamics of the phosphatidylcholine and the phosphatidylethanolamine head group in L-M fibroblasts as studied by deuterium nuclear magnetic resonance. *EMBO J.* **1987**, *6*.
- (87) Ferreira, T. M.; Coreta-Gomes, F.; Ollila, O. H. S.; Moreno, M. J.; Vaz, W. L. C.; Topgaard, D. Cholesterol and POPC segmental order parameters in lipid membranes:

solid state ^1H - ^{13}C NMR and MD simulation studies. *Phys. Chem. Chem. Phys.* **2013**, *15*, 1976–1989.

- (88) Ollila, O. S.; Pabst, G. Atomistic resolution structure and dynamics of lipid bilayers in simulations and experiments. *Biochimica et Biophysica Acta (BBA) - Biomembranes* **2016**, *1858*, 2512 – 2528.
- (89) Ferreira, T. M.; Sood, R.; Bärenwald, R.; Carlström, G.; Topgaard, D.; Saalwächter, K.; Kinnunen, P. K. J.; Ollila, O. H. S. Acyl Chain Disorder and Azelaoyl Orientation in Lipid Membranes Containing Oxidized Lipids. *Langmuir* **2016**, *32*, 6524–6533.
- (90) Catte, A.; Girych, M.; Javanainen, M.; Loison, C.; Melcr, J.; Miettinen, M. S.; Monticelli, L.; Maatta, J.; Oganesyan, V. S.; Ollila, O. H. S. et al. Molecular electrometer and binding of cations to phospholipid bilayers. *Phys. Chem. Chem. Phys.* **2016**, *18*, 32560–32569.
- (91) Melcr, J.; Martinez-Seara, H.; Nencini, R.; Kolafa, J.; Jungwirth, P.; Ollila, O. H. S. Accurate Binding of Sodium and Calcium to a POPC Bilayer by Effective Inclusion of Electronic Polarization. *The Journal of Physical Chemistry B* **2018**, *122*, 4546–4557.
- (92) Ollila, O. H. S. CHARMM36 simulations of POPC mixed with cationic surfactant. 2018; <https://doi.org/10.5281/zenodo.1288297>.
- (93) Melcr, J. POPC lipid membrane, 303K, Charmm36 force field, simulation files and 200 ns trajectory for Gromacs MD simulation engine v5.1.2. 2016; <https://doi.org/10.5281/zenodo.153944>.
- (94) Favela-Rosales, F. MD simulation trajectory of a lipid bilayer: Pure POPC in water. SLIPIDS, Gromacs 4.6.3. 2016. 2016; <https://doi.org/10.5281/zenodo.166034>.
- (95) Hauser, H.; Shipley, G. G. Interactions of monovalent cations with phosphatidylserine bilayer membranes. *Biochemistry* **1983**, *22*, 2171–2178.

- (96) Hauser, H.; Shipley, G. Comparative structural aspects of cation binding to phosphatidylserine bilayers. *Biochimica et Biophysica Acta (BBA) - Biomembranes* **1985**, *813*, 343 – 346.
- (97) Mattai, J.; Hauser, H.; Demel, R. A.; Shipley, G. G. Interactions of metal ions with phosphatidylserine bilayer membranes: effect of hydrocarbon chain unsaturation. *Biochemistry* **1989**, *28*, 2322–2330.
- (98) Cevc, G. Membrane electrostatics. *Biochim. Biophys. Acta - Rev. Biomemb.* **1990**, *1031*, 311 – 382.
- (99) Kim, S.; Patel, D.; Park, S.; Slusky, J.; Klauda, J.; Widmalm, G.; Im, W. Bilayer Properties of Lipid A from Various Gram-Negative Bacteria. *Biophysical Journal* **2016**, *111*, 1750 – 1760.
- (100) Nencini, R. Simulation data for CHARMM36 POPC bilayer, 100 lipids/leaflet, 310K, GROMACS 5.1.4. 2018; <https://doi.org/10.5281/zenodo.1198158>.
- (101) Nencini, R. Simulation data for CHARMM36 POPC bilayer, 100 lipids/leaflet, 450 mM CaCl₂ ("NB-Fix" used), 310K, GROMACS 5.1.4. 2018; <https://doi.org/10.5281/zenodo.1198171>.
- (102) Javanainen, M. POPC @ 310K, 450 mM of CaCl₂. Charmm36 with default Charmm ions. 2016; <http://dx.doi.org/10.5281/zenodo.51185>.